

**WPSA Report**

**CREATE/IST**

**Coupling of the CCS reconstruction code and of  
the FBC controller with the CREATE  
control-oriented simulation tools**

*D. Corona, G. De Tommasi, M. Mattei, A. Mele, A. Pironti*

*with contributions of*

*Y. Miyata, T. Suzuki, H. Urano*

# Table of Contents

|   |           |
|---|-----------|
| <u>1. BENCHMARK OF CCS WITH CREATE-NL EQUILIBRIUM CODE</u>  | <u>4</u>  |
| <u>2. JT-60SA MAGNETIC CONTROL SIMULATION ENVIRONMENT</u>   | <u>5</u>  |
| <u>3. CLOSED-LOOP SIMULATION OF THE CREATE CONTROL ARCHITECTURE BY USING CCS CODE</u>                         | <u>8</u>  |
| <u>4. ASSESSMENT OF THE PLASMA SHAPE CONTROL PERFORMANCE USING CCS</u>  | <u>15</u> |
| 4.1 REFERENCE SCENARIOS FOR ASSESSMENT  | 16        |
| 4.2 RESULTS OF THE PERFORMANCE ASSESSMENT   | 18        |
| 4.2.1 RESPONSE TO A MINOR DISRUPTION  | 18        |
| 4.2.2 RESPONSE TO A CHANGE IN SHAPE   | 25        |
| 4.2.3 PRELIMINARY ASSESSMENT IN PRESENCE OF NOISE   | 27        |
| <u>5. INTEGRATION OF THE QST MAGNETIC (FBC) CONTROLLER AND CCS RECONSTRUCTION TO THE CREATE MODEL OF JT60</u> | <u>28</u> |
| <u>6. REFERENCES</u>  | <u>31</u> |

# Simulations of the JT-60SA magnetic control system and integration of the CCS reconstruction code

This report describes the activities that have been carried out to include the Cauchy Condition Surface (CCS) reconstruction code provided by the JT-60SA team in a control-oriented simulation scheme based on the CREATE modelling tools. In the provided simulation setup, the fluxes reconstructed by CCS at the selected control points are fed back to an *isoflux* controller designed using the eXtreme Shape Controller (XSC) approach, to track the desired plasma shape.

The result of the assessment of the XSC-like controller using CCS are also presented.

Moreover, the report shows also the results of the coupling of the QST plasma shape, position and current controller (FBC) with the CREATE plasma/circuits linear model.

This report is structured as follows:

- In Section 1, the results of the comparison between the plasma boundary reconstruction made by CCS and by the CREATE-NL nonlinear equilibrium code is presented. The JT-60SA Scenario 2 at the start of flattop has been considered for this comparison.
- Section 2 introduce the control-oriented simulation environment used to couple the CREATE tools with the QST codes. A first comparison between the CCS output and of the output of the CREATE linear model is presented.
- Section 3 describes the setup for closed-loop simulations in the proposed control-oriented simulation environment and shows some preliminary results obtained feeding back the fluxes computed by CCS to the *isoflux* controller proposed in [2], when the minor disruption defined in [1] is considered.
- Section 4 summarizes the results of the performance assessment of the controller XSC-like *isoflux* controller using CCS. The assessment has been performed against several test scenarios, similarly to what has been done in [3]. Moreover, a preliminary assessment of the effect of measurement noise on plasma shape controller is also presented.
- Section 5 shows the results obtained by running closed-loop simulation with FBC controller and the CREATE plasma/circuits linear model.

## 1. Benchmark of CCS with CREATE-NL equilibrium code

A plasma equilibrium was generated using the CREATE-NL modelling tool. The Start of Flattop (SOF) snapshot at 18.66 s for the Scenario 2 specified in [1] has been considered to compare the CREATE-NL and CCS outputs. To run such a comparison, the CREATE-NL code has been configured to include among its outputs the fields and fluxes for the set of magnetic probes specified in the geo.in file of the CCS code. The fluxes and fields outputs of CREATE-NL, together with the values of the plasma current and of the currents in the CS, EF and FPPC coils, have been given as inputs to the CCS code. A comparison between the last closed flux surfaces (LCFSs) computed by both CREATE-NL and CCS for the considered scenario snapshot is shown in Figure 1; in the same figure, the position of the considered flux and field probes is shown.

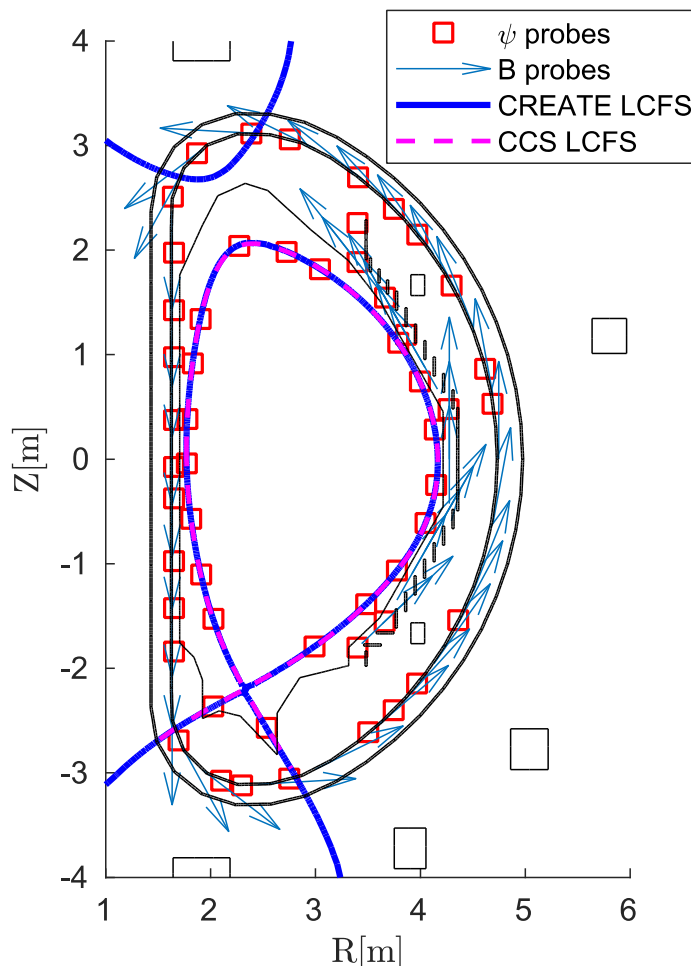


**FIGURE 1. SOF EQUILIBRIUM RECONSTRUCTED FROM CREATE-NL AND THE CCS CODES AND LOCATION OF MAGNETIC FIELD AND FLUX SENSORS**

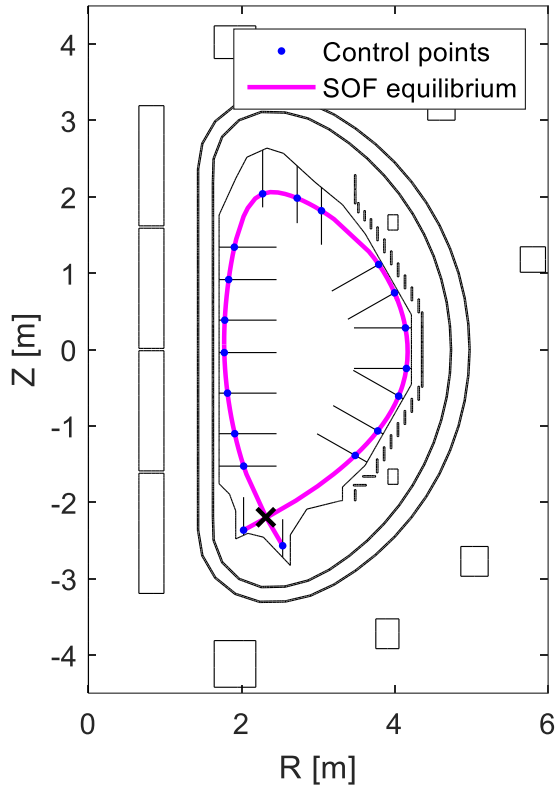


**FIGURE 2. LCFS FOR SCENARIO 2 SOF EQUILIBRIUM. IN THIS FIGURE THE 19 SELECTED CONTROL POINTS FOR PLASMA SHAPE CONTROL ARE ALSO SHOWN.**

## 2. JT-60SA Magnetic Control Simulation Environment

To perform closed-loop simulations, the output of a CREATE-L plasma/circuits linearized model was fed as input to the CCS reconstruction code. The CCS reconstruction code receives the following inputs from the JT60-SA linearized model:

- the plasma current;
- the value of the current flowing in active circuits, i.e., in the superconductive CS and EF coils, and in the two in-vessel copper coils (FPPCs);
- the measurements of the magnetic probes.

After its execution, the CCS reconstruction code gives as outputs the fluxes at the selected control points and the position and flux at the X-point. It is worth to remark that the version of the CCS code provided by the JT-60SA team permits to select a maximum of 19 flux control points (Figure 2 shows the location of the selected points).

According to the workflow described above, a Simulink scheme (whose simplified diagram is shown in Figure 3) was set up to simulate the magnetic control system of JT-60SA. The magnetic control system includes the Vertical Stabilization controller (which exploits the FPPCs as actuators), the controller for the current flowing in the Poloidal Field Circuits (PFC Control), the Plasma Current control and Shape control. For this report, an *isoflux* algorithm has been adopted to control the plasma boundary (see also [2]). However, the proposed control architecture also supports a *gap-based* control algorithm, as it was described in [3].

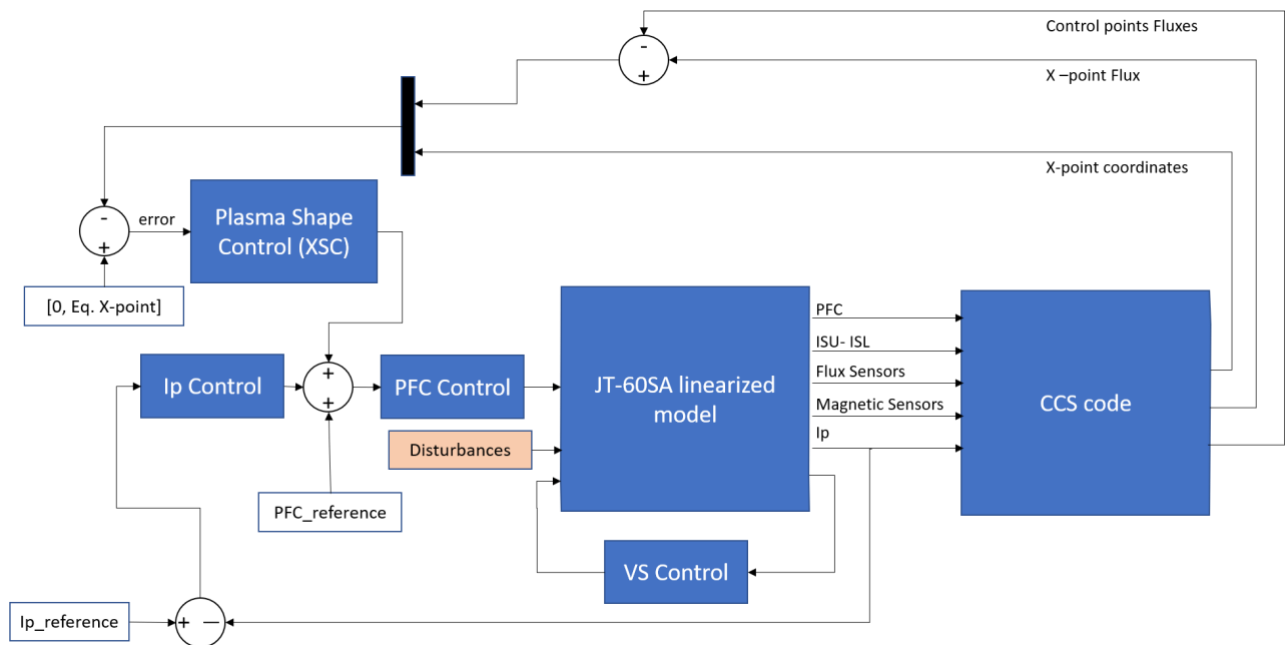


**FIGURE 3. SIMULATION SCHEME USED TO INCLUDE THE CCS CODE IN THE CONTROL ARCHITECTURE PROPOSED IN [2].**

The assessments of the control architecture proposed in [2] are summarized in Section 3.

Further closed-loop simulations have been performed by replacing the control algorithms shown in Figure 3 with the FBC controller, and by using again the CREATE linearized model to mimic the plant behavior. More in detail, the output current requests for the CS and EF coils have been fed as input to the PFC controller, while the current request for the FPPC coils have been directly fed to the model, where the FPPC circuit was set in *current-driven* mode. The results of this coupling are discussed in Section 5.

A preliminary simulation has been carried out to compare the CCS and the CREATE linear model outputs. More in details, a linearized model of JT-60SA for Scenario 2 at the SOF with the presence of a *minor disruption*, as it has been described in [1]. As far as magnetic control is concerned, a minor

disruption can be modeled by a variation of both poloidal beta  $\beta_p$  and plasma internal inductance  $l_i$ , according to the time traces reported in Figure 4.

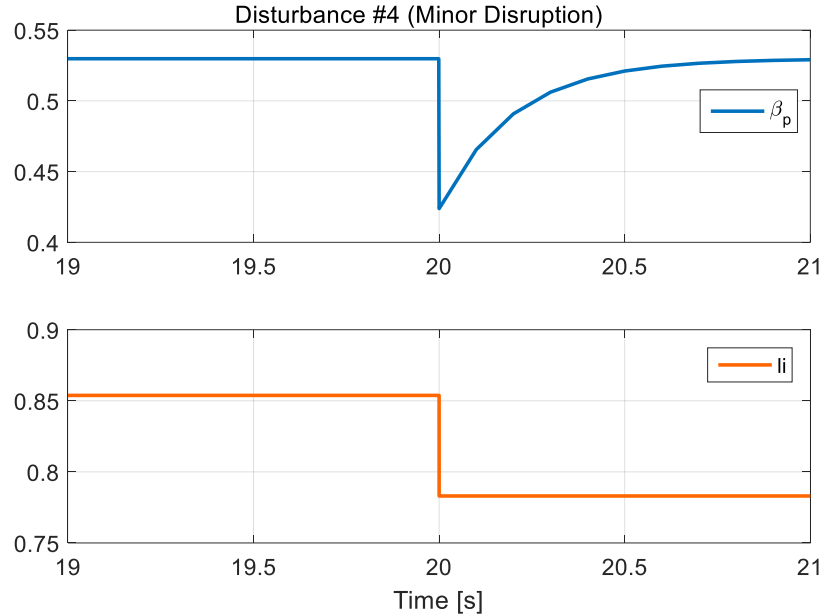


**FIGURE 4. POLOIDAL BETA  $\beta_p$  AND PLASMA INTERNAL INDUCTANCE  $l_i$  TIME BEHAVIOUR CORRESPONDING TO A MINOR DISRUPTION, AS DESCRIBED IN [1].**

This preliminary test has been performed by integrating the CCS code in the Simulink in open-loop, i.e., without feeding back its output to the magnetic controller. The same controller presented in [3] was used, and the outputs of the probes specified in the `geo.in` file of the CCS were added to the linear model outputs. These outputs were fed to the CCS, to enable the comparison of the reconstructed fluxes at the controlled points and at the X-point. Figure 5 shows a comparison between the flux at the X-point as it was reconstructed by both the CREATE linear model and the CCS method. A slight difference in the values obtained with the two approaches can be noticed, whose origin is to be found in the different numerical methods used to reconstruct the flux.

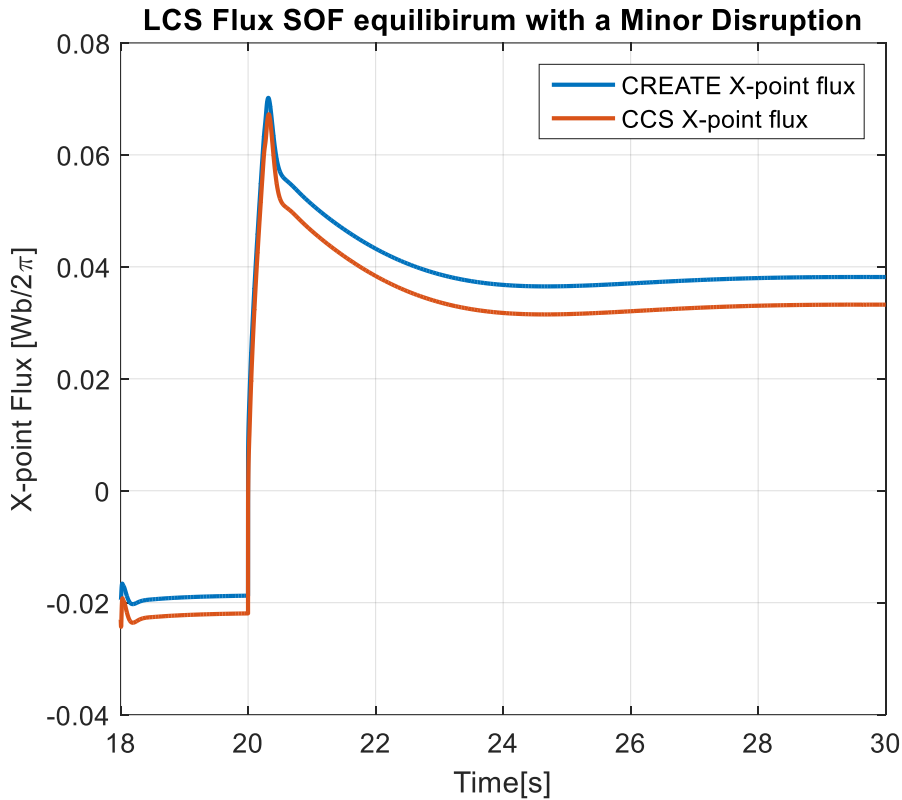


FIGURE 5. FLUX AT THE X-POINT COMPUTED BY THE CREATE LINEAR MODEL AND CCS RECONSTRUCTIONS CODE.

### 3. Closed-loop simulation of the CREATE control architecture by using CCS code

Once the open-loop validation described in Section 2 was performed, the CCS algorithm was used in closed-loop simulation to generate the feedbacks for a *XSC-like* isoflux controller, which has been designed following the approach presented in [2]. The CCS code was executed with a sampling time of 1 ms. At each simulation step, the outputs of the JT-60SA linear model needed by the CCS are written in the `fort.70` file, and then the CCS is invoked in Simulink, by using a Matlab function. The CCS then writes its outputs in the `fort.71` file, whose content is read, to feed the XSC with the value of the flux at the control points. It should be noticed that, this data exchange via ASCII files has a negative impact on the time needed to perform relatively low demanding simulations. Such a limitation could be overcome in future by compiling the CCS code (and the FBC) as Simulink s-functions.

Figures 6-14 summarize the preliminary results aimed at verifying the correct integration of the CCS code in the CREATE simulation environment. As for the open-loop validation, also in the closed-loop case reported in this section, the minor disruption defined in [1], whose corresponding poloidal beta and internal inductance behaviour are reported in Figure 4, has been used as test scenario.

### SOF equilibrium with a Minor Disruption (CCS reconstruction)

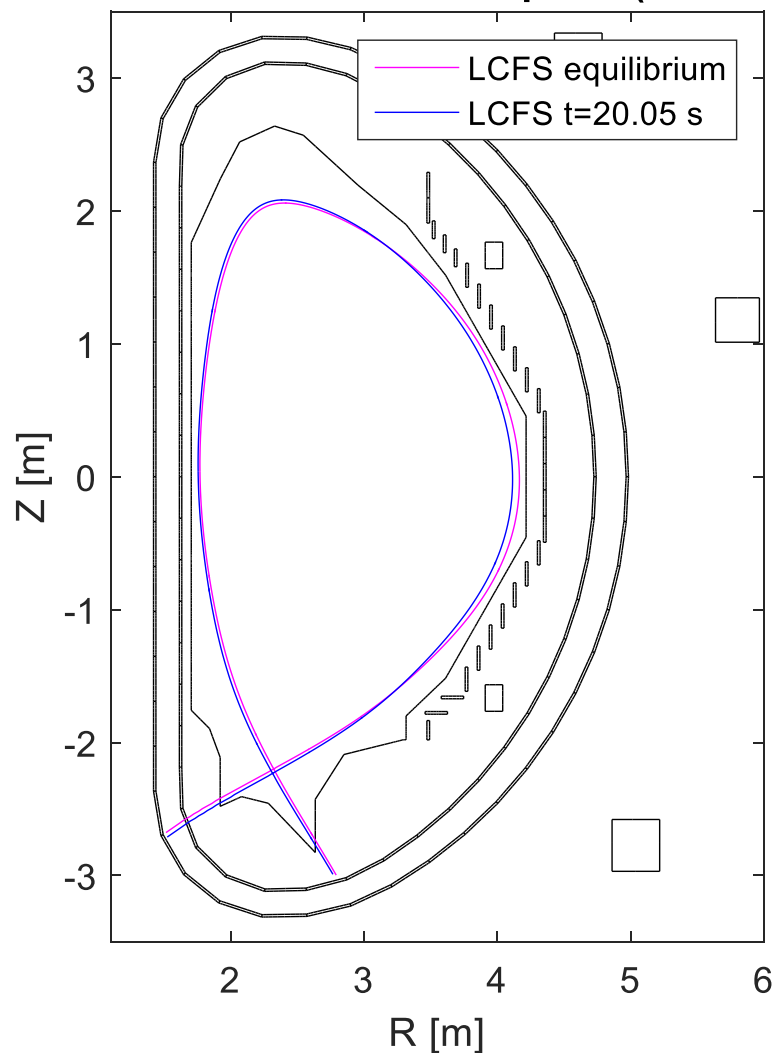


**FIGURE 6. COMPARISON BETWEEN THE CCS RECONSTRUCTION OF THE LCFS AT THE EQUILIBRIUM AND AT T=20.05 s, I.E., 50 MS AFTER THE DISTURBANCE SHOWS UP.**

## SOF equilibrium with a Minor Disruption (CREATE reconstruction)

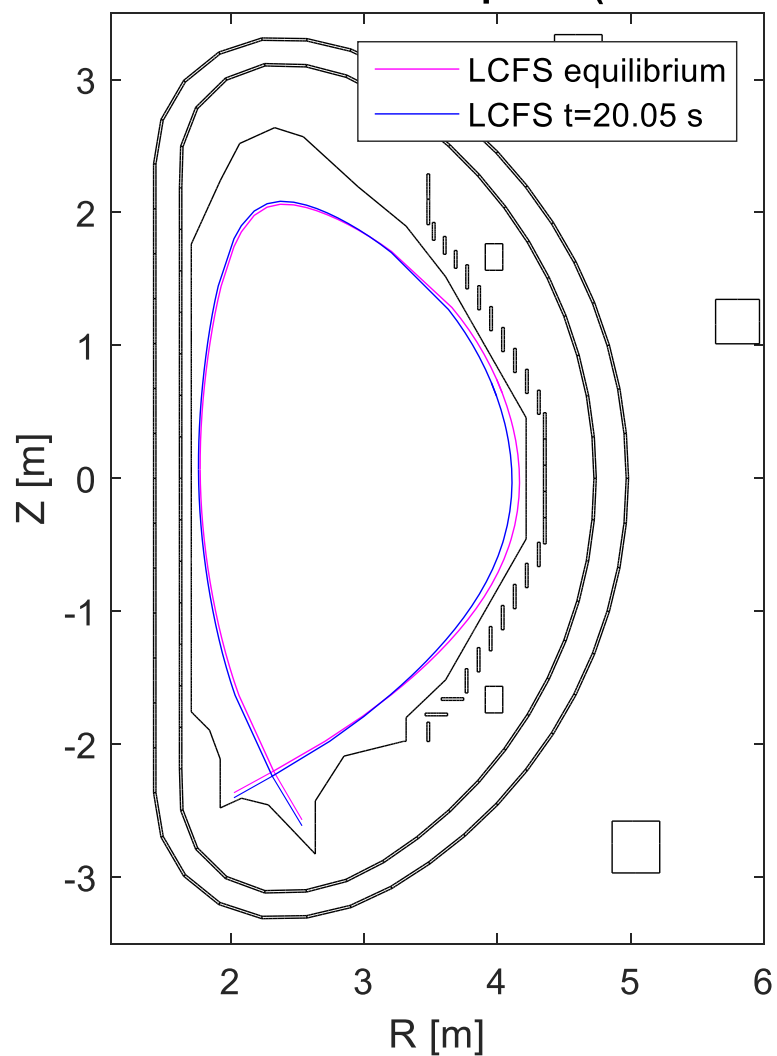


**FIGURE 7. COMPARISON BETWEEN THE CREATE RECONSTRUCTION OF THE LCFS AT THE EQUILIBRIUM AND AT T=20.05 s, I.E., 50 MS AFTER THE DISTURBANCE SHOWS UP.**

### SOF equilibrium with a Minor Disruption (Steady State)

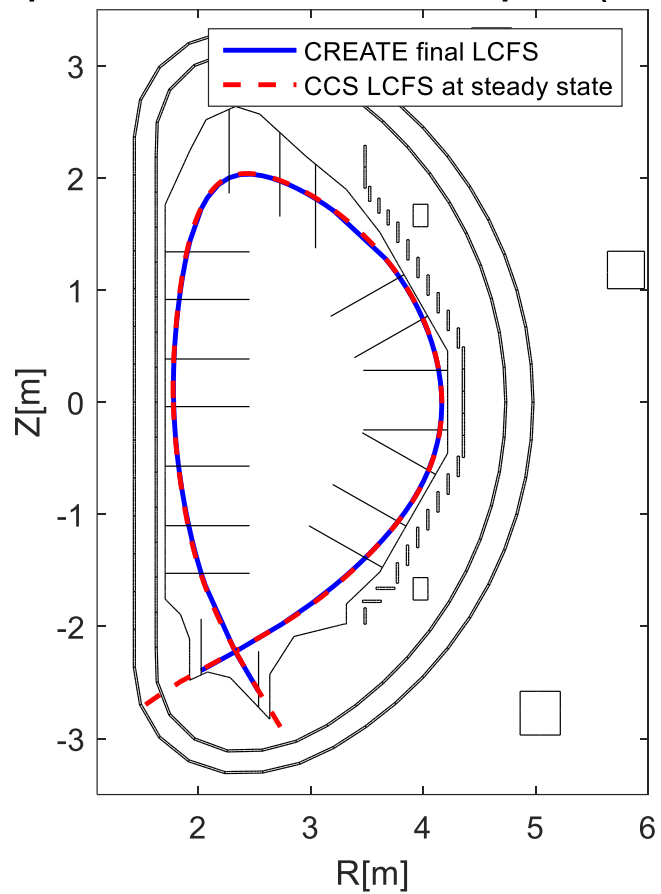


**FIGURE 8. COMPARISON BETWEEN THE LCFS OBTAINED BY THE CREATE LINEAR MODEL AND THE CCS RECONSTRUCTION CODE AT STEADY-STATE. IT CAN BE NOTICED THAT THE TWO RECONSTRUCTIONS ARE IN VERY GOOD AGREEMENT.**

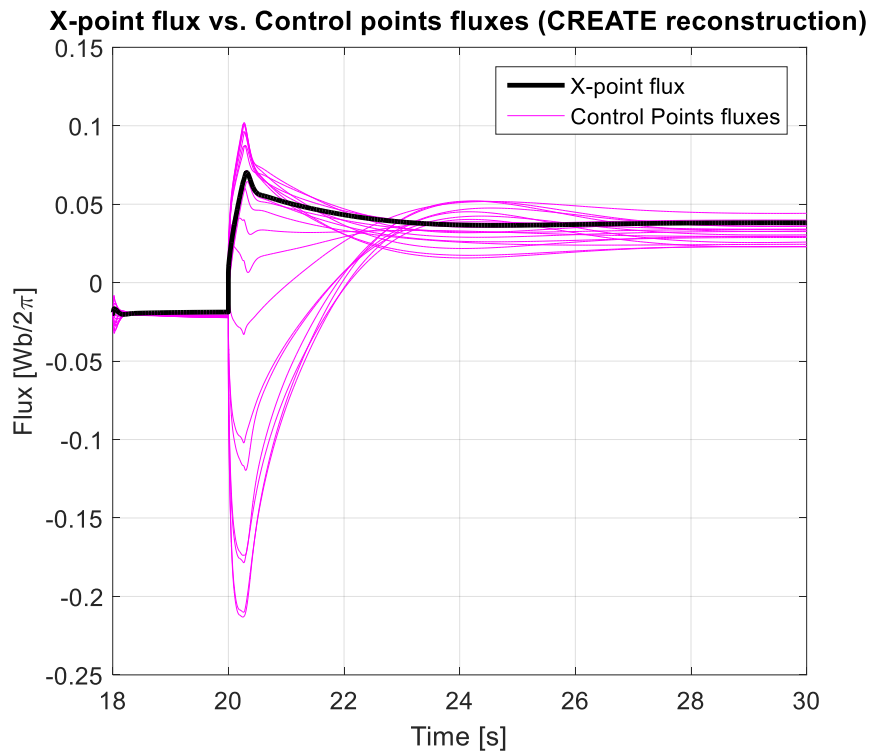


**FIGURE 9. COMPARISON BETWEEN THE FLUX AT THE X-POINT AND THE FLUXES AT 19 THE CONTROL POINTS RECONSTRUCTED BY THE CREATE TOOLS. NOTE THAT THIS ARE NOT THE VARIABLES FED BACK INTO THE CONTROLLER.**

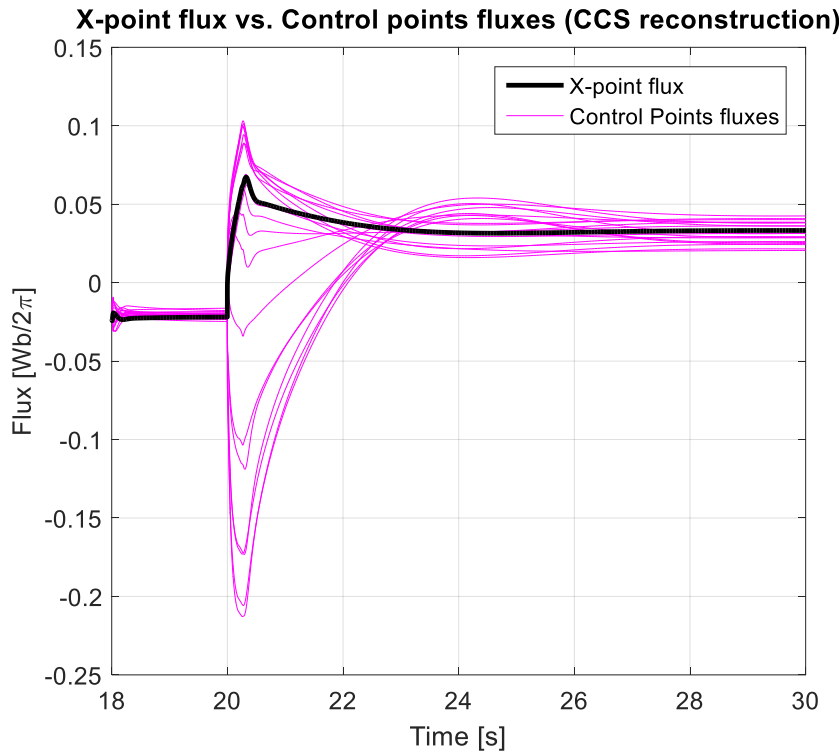


**FIGURE 10. COMPARISON BETWEEN THE FLUX AT THE X-POINT AND THE FLUXES AT 19 THE CONTROL POINTS RECONSTRUCTED BY THE CCS ALGORITHM. THIS ARE THE VARIABLES USED BY THE PROPOSED ISOFLUX PLASMA SHAPE CONTROLLER.**

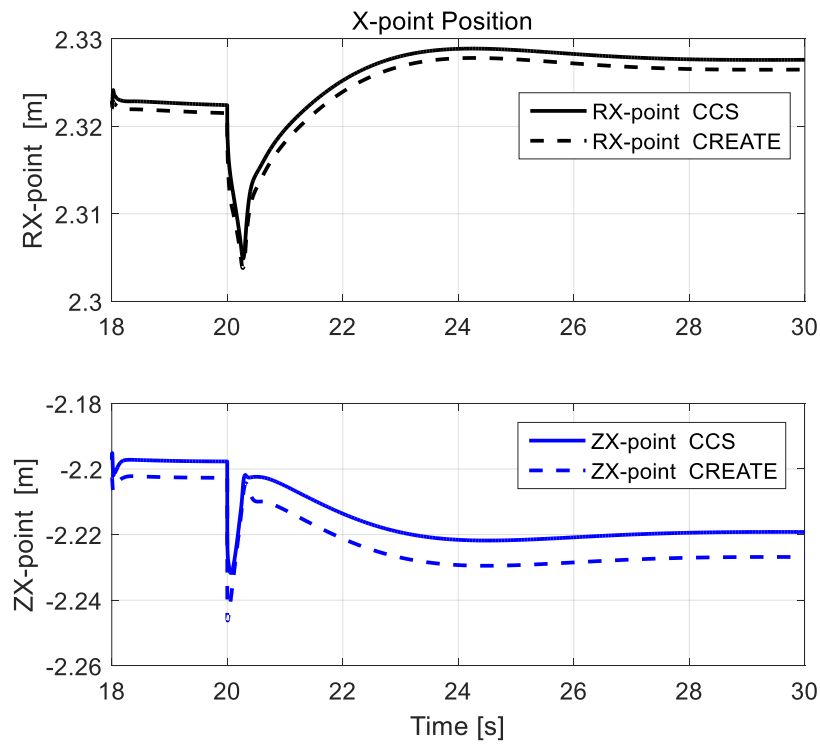


**FIGURE 11. X-POINT RADIAL AND VERTICAL POSITIONS RECONSTRUCTED WITH CCS AND CREATE.**

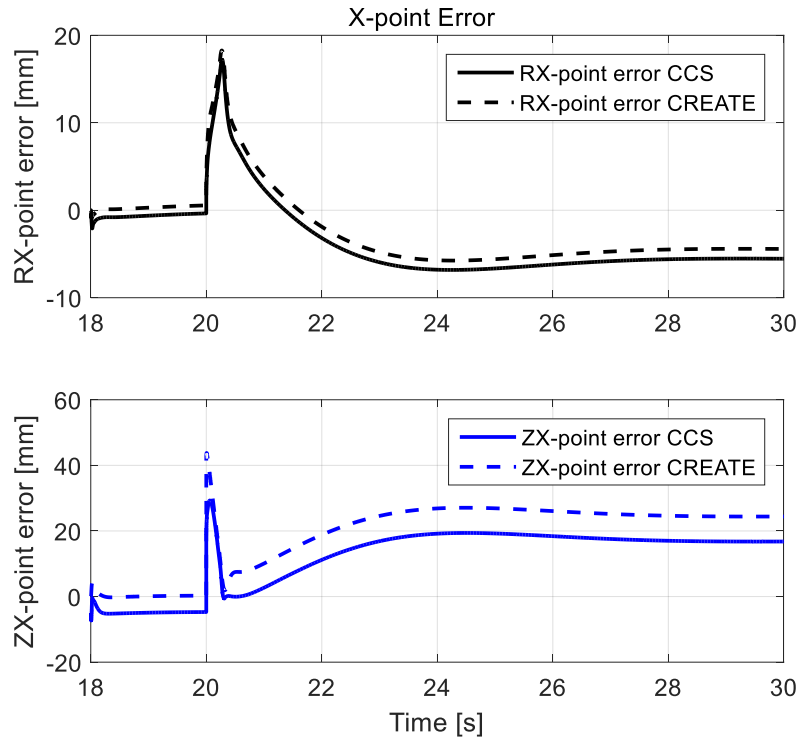


**FIGURE 12. CONTROL ERROR ON THE X-POINT RADIAL AND VERTICAL POSITIONS.**

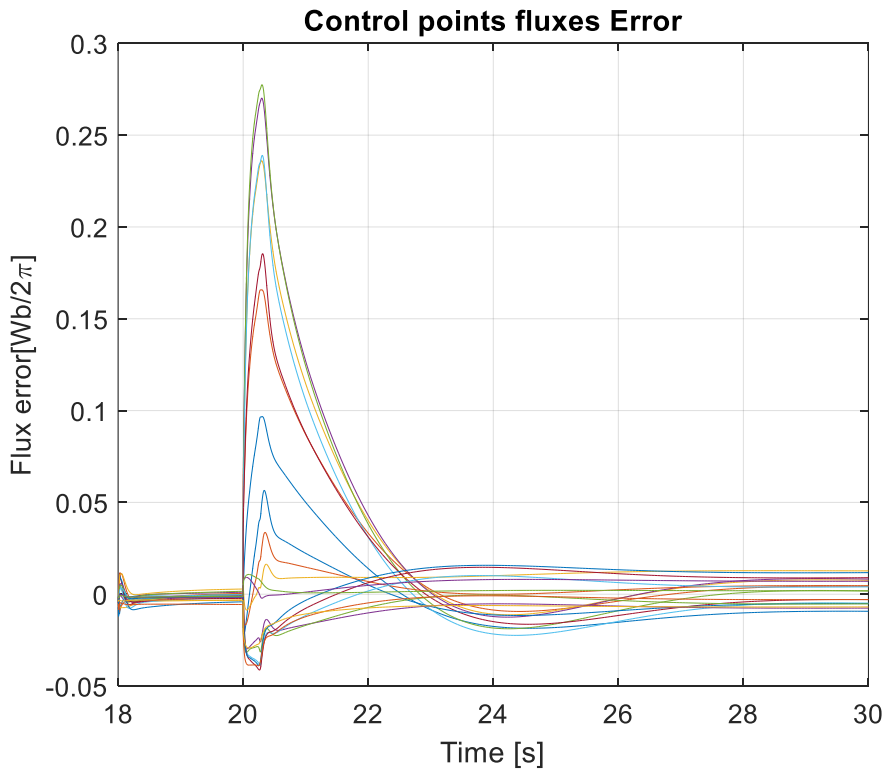


**FIGURE 13. CONTROL ERROR AT THE 19 CONTROL POINTS.**

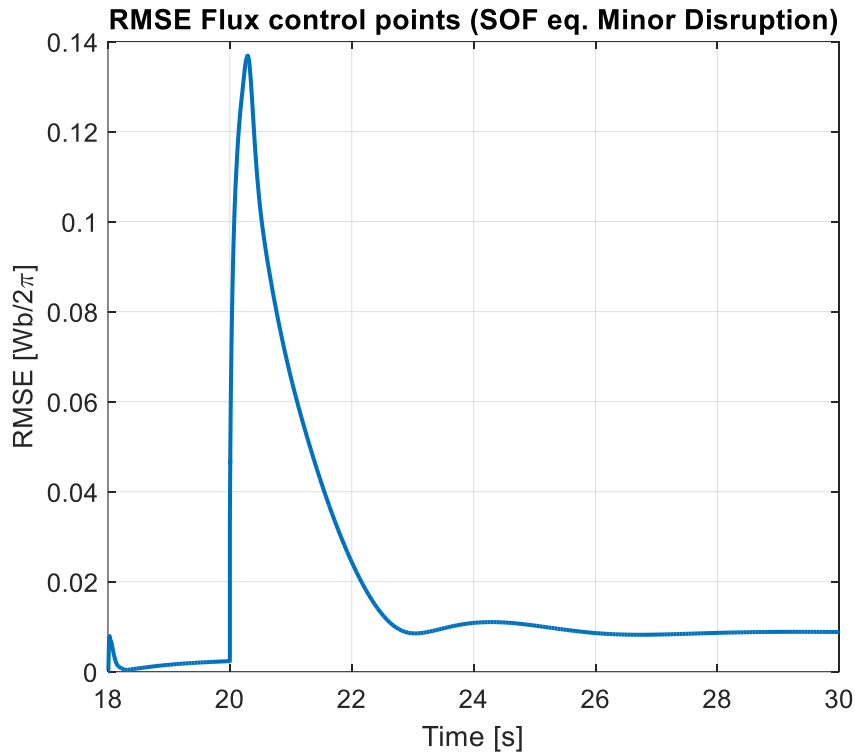


**FIGURE 14. TIME TRACE OF THE ROOT-MEAN-SQUARE ERROR (RMSE) COMPUTED ON THE SELECTED CONTROL POINTS.**

#### 4. Assessment of the plasma shape control performance using CCS

In this section, the result of the performance assessment of the *isoflux-based* plasma shape controller designed using the procedure presented in [2] are summarized.

In the following, the performance of the shape controller is evaluated as a function of the number of controlled segments for several test scenarios, similarly to what has been done in [3] in the case of a *gap-based* plasma shape controller. Moreover, a preliminary assessment of the effect of measurement noise on plasma shape controller by using CCS in closed-loop simulation, is also presented. The latter analysis shows that, under the current assumptions, measurement noise will not be an issue for plasma shape control.

#### 4.1 Reference scenarios for assessment

The following scenarios have been considered to assess the performance of the proposed XSC-like isoflux controller by using CCS to reconstruct the flux map starting from the magnetic measurement simulated by the CREATE linear model:

1. the minor disruption defined in [1] ( $\beta_p$  and  $l_i$  time traces shown in Figure 4);
2. the disturbance expected at the end of the ramp-up phase, as defined in [4] (see Disturbance #1 in Figure 15 for the corresponding  $\beta_p$  and  $l_i$  time traces);
3. the compound ELM defined in [1] (see Disturbance #2 in Figure 15 for the corresponding  $\beta_p$  and  $l_i$  time traces);
4. a minor disruption obtained by scaling the time traces proposed for ITER in [5] and [6] (see Figure 16). Note that, although this may be not realistic for JT-60SA from the physics point view, it has been considered to extend the number of test cases;
5. the change in the shape reference, starting from the SOF shape and then reducing the top area of the LCFS.

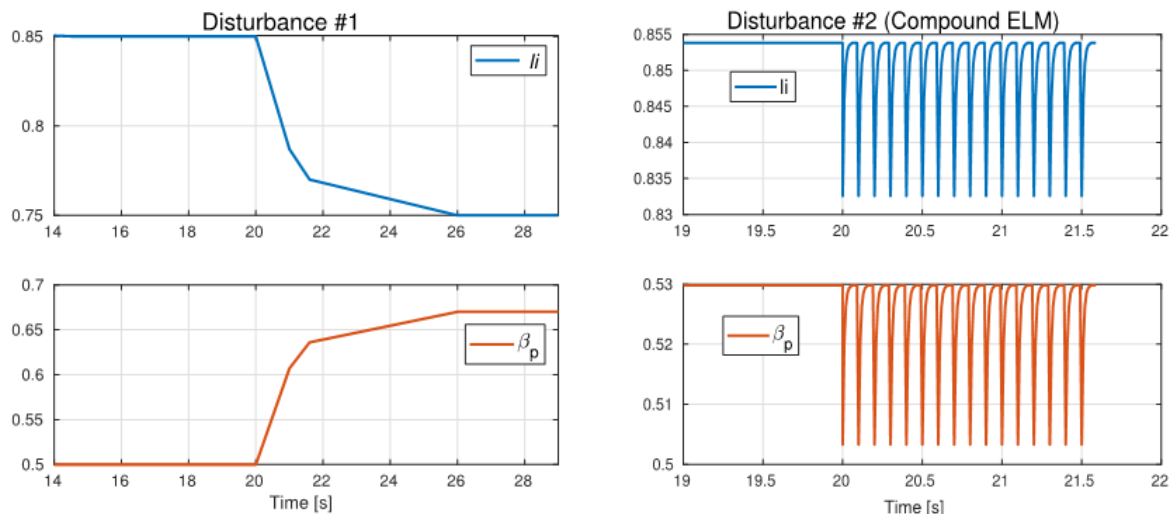


**FIGURE 15. DISTURBANCE #1 BASED ON THE DEFINITION TAKEN FROM [4] AND DISTURBANCE #2 BASED ON THE DEFINITION OF COMPOUND ELM GIVEN IN [1].**

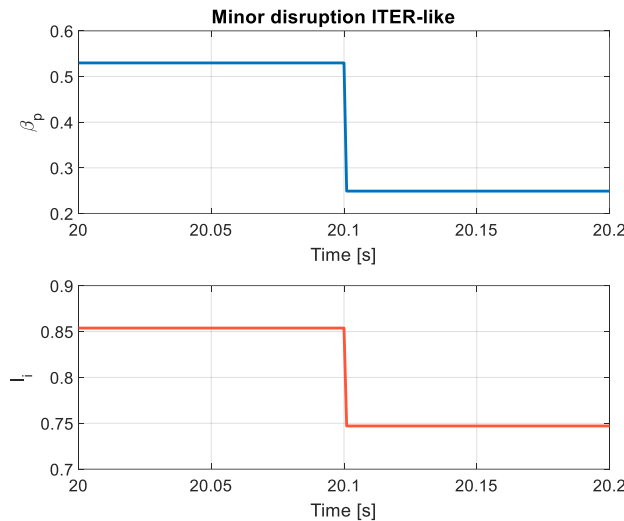


**FIGURE 16. MINOR DISRUPTION OBTAINED BY SCALING THE DEFINITION GIVEN IN [5] AND [6].**

Since the CCS code only allows a maximum of 19 control points, in addition to that control segments shown in Figure 2, the set of control segments proposed both in [7] and [8] were also considered (see Figure 17).

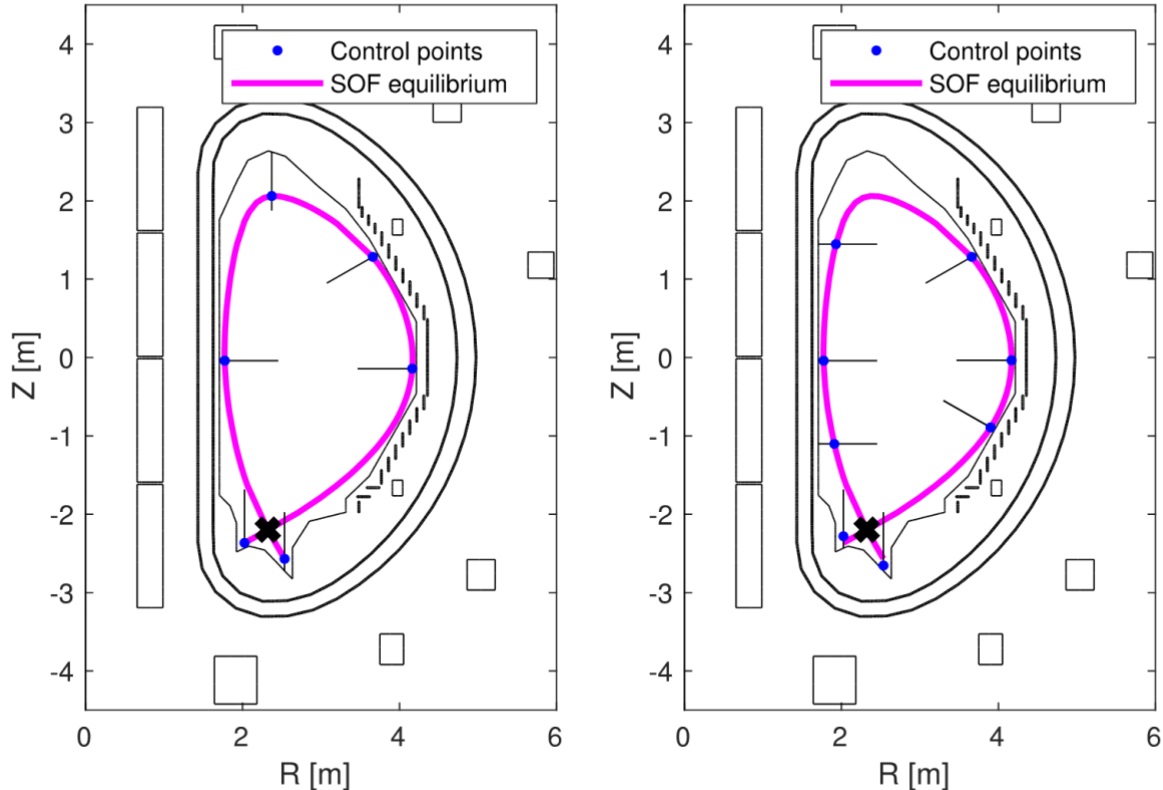


**FIGURE 17. CONTROL SEGMENTS CONSIDERED IN [7] (LEFT SIDE) AND [8] (RIGHT SIDE).**

## 4.2 Results of the performance assessment

### 4.2.1 Response to a minor disruption

As far as the disturbance rejection is concerned, this report focuses on the minor disruption case, since this represents the worst case, even during the transients (similarly to what has been presented in [3], where the performance of gap-based shape controller was assessed). In this section we present the simulation results for both the minor disruption defined in [1] and the one given by scaling the definition given [5], [6].

#### 4.2.1.1 Minor disruption defined in [1]

The comparison of the LCFS at steady-state, i.e., after the disturbance is rejected, is shown in Figure 18, where the comparison for three different selections of control segments is shown. It can be noticed that there are no significant differences between the reconstruction made by the CREATE linear model and the one made by the CCS code (the latter being the one controlled in feedback in the considered simulation setup).

Due to the not remarkable difference at sight in the LCFS results for the 19 and 6 control segments cases, Figure 19 shows the worst case for the steady-state error in the presence of a minor disruption, which is the one obtained for the 8 control segments case (see also Table 1).

Moreover, Figure 20 shows the time traces for the fluxes at the 8 control points and at the X-point, while Figure 21 shows the correspondent flux control errors. Figure 22 shows the maximum deviation in shape for the case of 8 control segments.

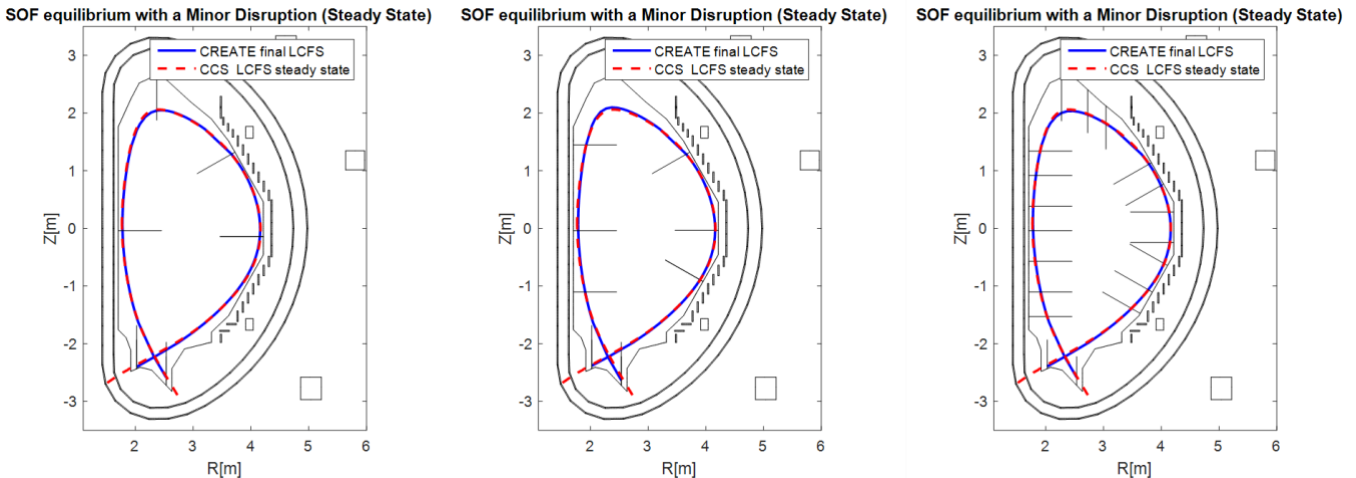


**FIGURE 18. LCFS RECONSTRUCTED BY CREATE AND CCS CODE FOR A SOF EQUILIBRIUM WITH A MINOR DISRUPTION AT STEADY-STATE FOR THE THREE CONSIDERED SELECTIONS OF CONTROL SEGMENTS.**

### SOF equilibrium with a Minor Disruption

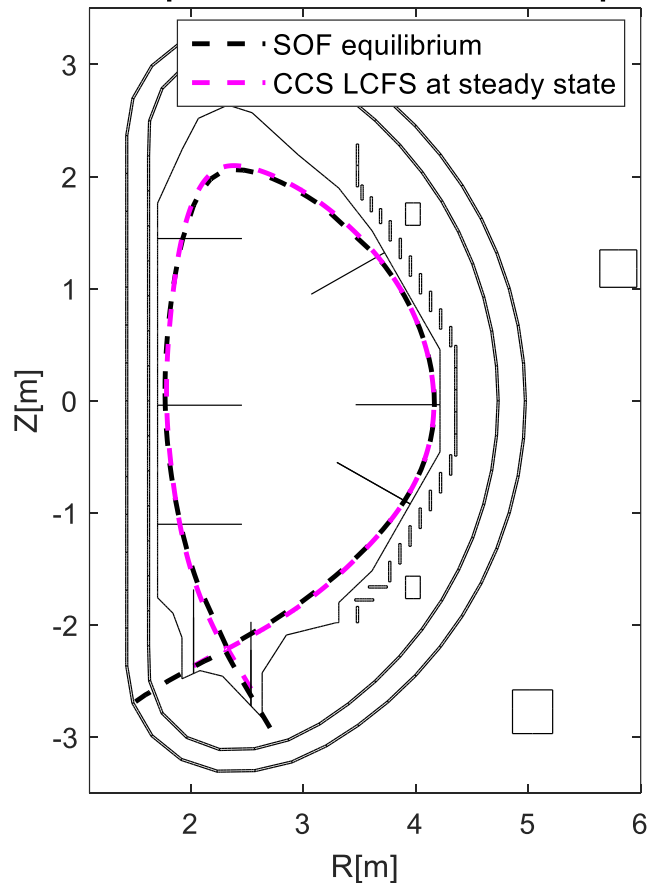


**FIGURE 19. COMPARISON BETWEEN THE REFERENCE SHAPE (I.E., THE SHAPE AT THE CONSIDERED EQUILIBRIUM) AND THE LCFS RECONSTRUCTED BY THE CCS CODE AT STEADY-STATE IN THE PRESENCE OF THE MINOR DISRUPTION DEFINED IN [1], WHEN 8 CONTROL SEGMENTS ARE CONSIDERED.**

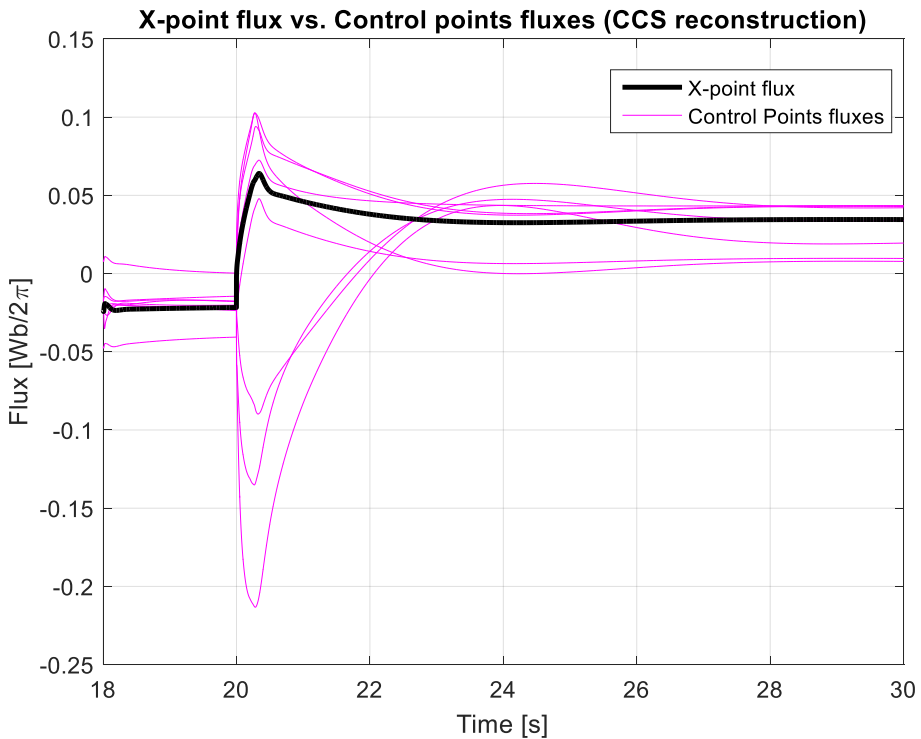


**FIGURE 20. COMPARISON BETWEEN THE FLUX AT THE X-POINT AND THE FLUXES AT THE 8 CONTROL POINTS RECONSTRUCTED BY THE CCS ALGORITHM, WHEN THE MINOR DISRUPTION DEFINED IN [1] IS APPLIED AT  $T = 20$  s.**

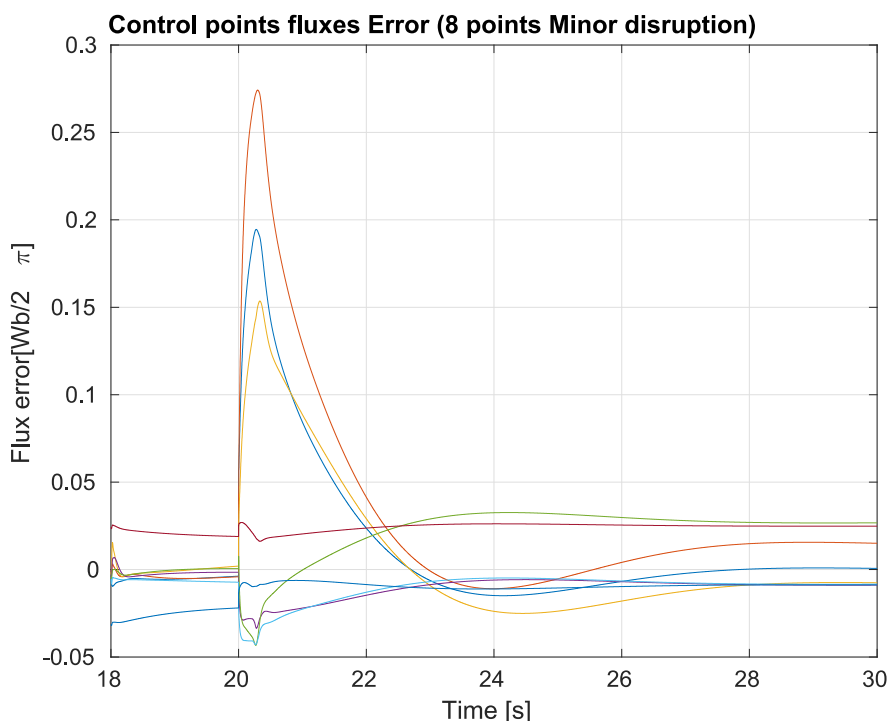


**FIGURE 21. FLUX CONTROL ERROR FOR THE CASE OF 8 CONTROL POINTS WHEN THE MINOR DISRUPTION DEFINED IN [1] IS APPLIED AT  $T=20$  s.**

## SOF equilibrium with a Minor Disruption (CCS, 8 control points)

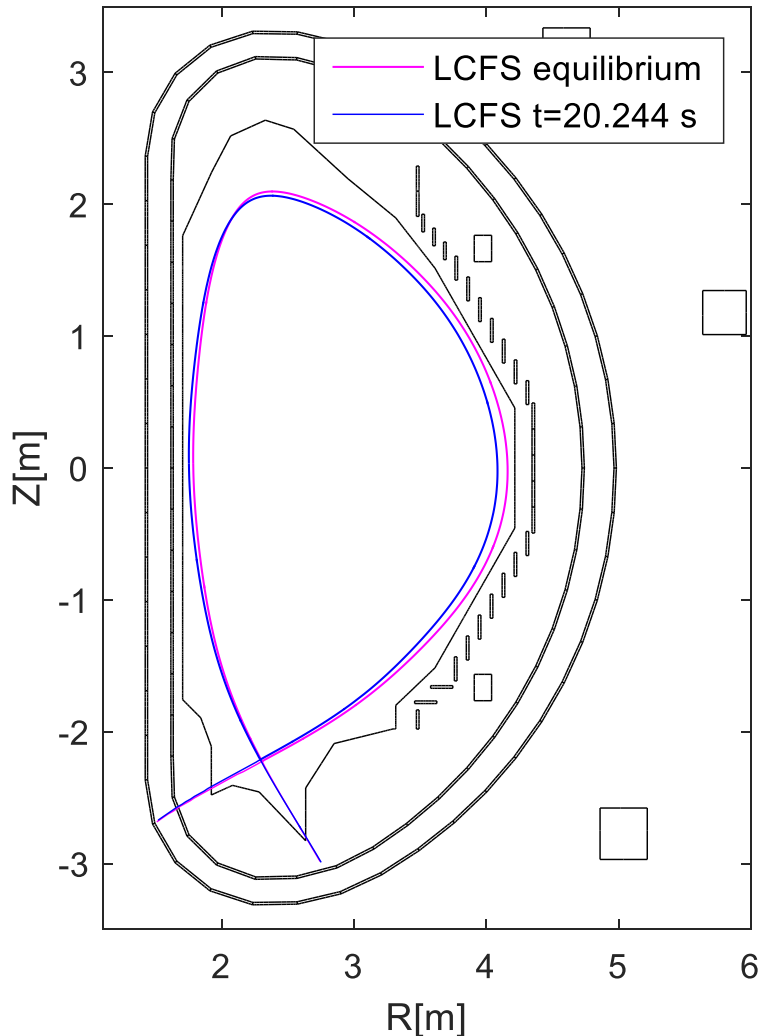


**FIGURE 22. MAXIMUM DEVIATION IN PLASMA SHAPE, WHEN THE MINOR DISRUPTION DEFINED IN [1] IS  
CONSIDERED AND 8 FLUXES ARE CONTROLLED.**

**TABLE 1 – FLUX ROOT-MEAN SQUARE ERROR (RMSE) AT STEADY-STATE FOR THE CONSIDERED DIFFERENT  
SELECTIONS OF CONTROL SEGMENTS, WHEN CCS CODE IS USED IN CLOSED-LOOP WHEN THE MINOR DISRUPTION  
DEFINED IN [1] IS CONSIDERED.**

| Number of control segments | Flux RMSE Steady-State [Wb/2π] |
|----------------------------|--------------------------------|
| 6 control segments         | 0.0121                         |
| 8 control segments         | 0.0152                         |
| 19 control segments        | 0.0069                         |

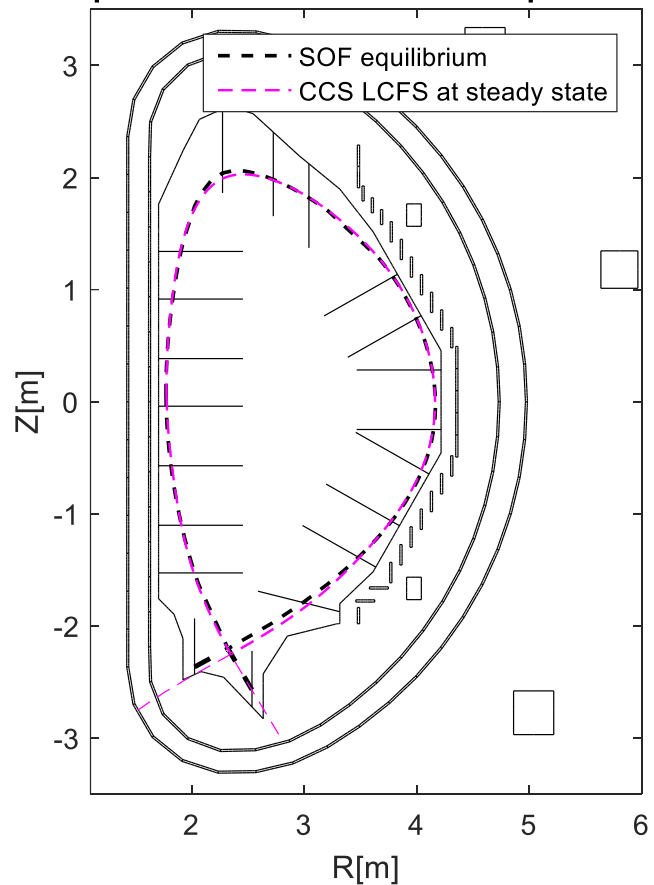
#### 4.2.1.2 ITER-like minor disruption

This section reports the results of the closed-loop simulation carried out with the XSC-like isoflux controller and the CCS code, in presence of an ITER-like minor disruption, obtained by scaling the poloidal beta and internal inductance time traces defined in [5] and [6]. Although such a disturbance may be not realistic from the physics point view, it has been considered as worst case for the plasma shape controller, since it turned out that it was the most challenging disturbance to reject among the one listed in Section 4.1.

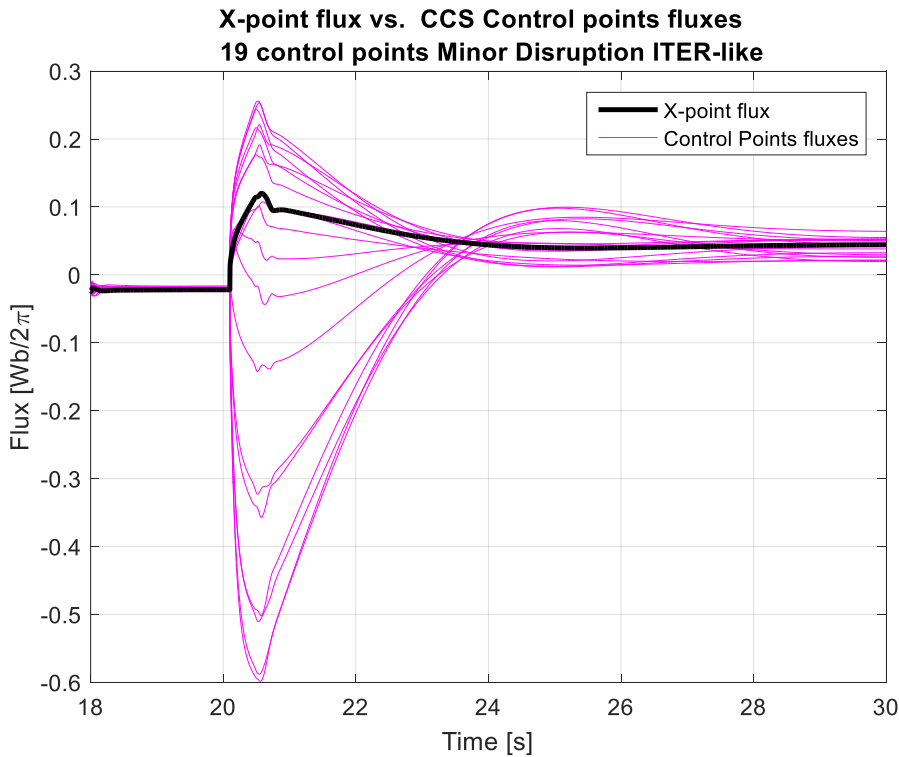
To effectively reject the ITER-like minor disruption, the XSC-like isoflux plasma shape controller controls to zero the flux differences at the 19 control points shown in Figure 2.

Figure 23 shows the deviation in shape at steady-state, while Figure 24 shows the time traces for the fluxes at the 19 control points, and Figure 25 shows the correspondent control errors. The maximum plasma shape deviation during the transient response is shown in Figure 26; it can be noticed that, among the considered cases, although the ITER-like minor disruption represents the worst case, the considered isoflux plasma shape controller is able to cope with it.

### SOF equilibrium with a Minor Disruption ITER-like



**FIGURE 23. COMPARISON BETWEEN THE REFERENCE SHAPE (I.E., THE SHAPE AT THE CONSIDERED EQUILIBRIUM) AND THE LCFS RECONSTRUCTED BY THE CCS CODE AT STEADY-STATE IN THE PRESENCE OF AN ITER-LIKE MINOR DISRUPTION, WHEN 19 CONTROL SEGMENTS ARE CONSIDERED.**



**FIGURE 24. COMPARISON BETWEEN THE FLUX AT THE X-POINT AND THE FLUXES AT THE 19 CONTROL POINTS RECONSTRUCTED BY THE CCS ALGORITHM, WHEN AN ITER-LIKE MINOR DISRUPTION IS APPLIED AT T=20 s.**

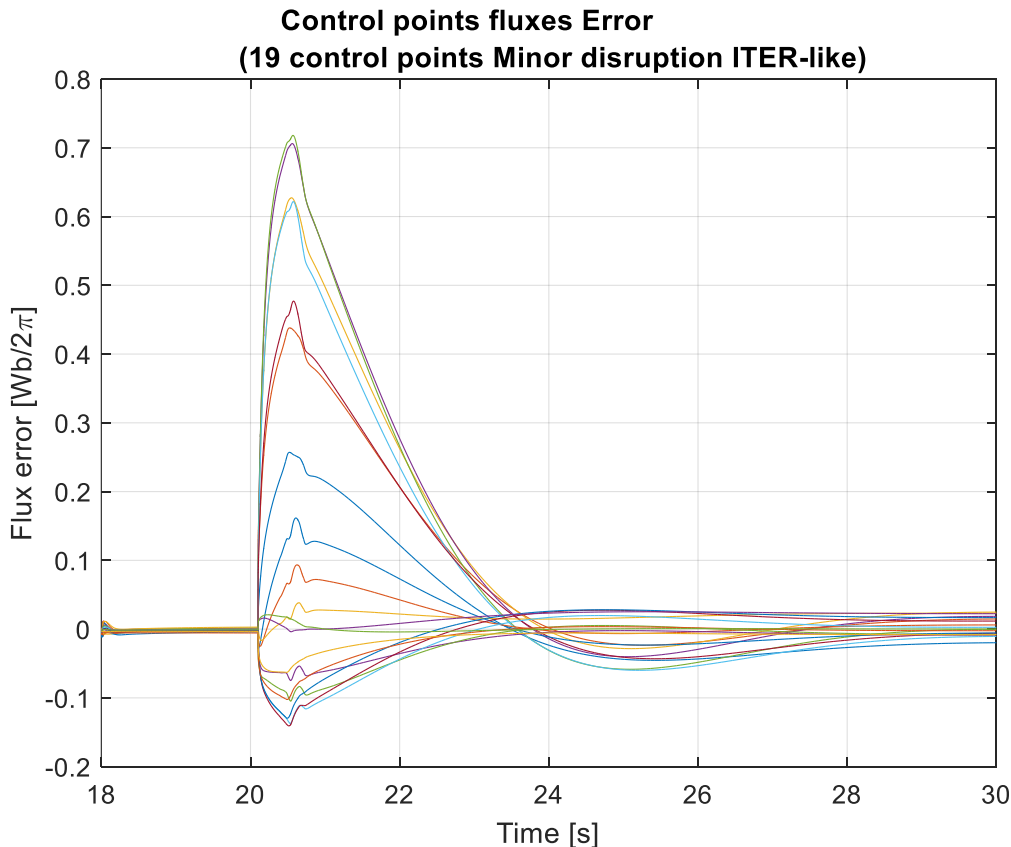


**FIGURE 25. FLUX CONTROL ERROR FOR THE CASE OF 19 CONTROL POINTS WHEN AN ITER-LIKE MINOR DISRUPTION IS APPLIED AT T=20 s.**

### SOF equilibrium with an ITER-like Minor Disruption 19 control points (CCS)

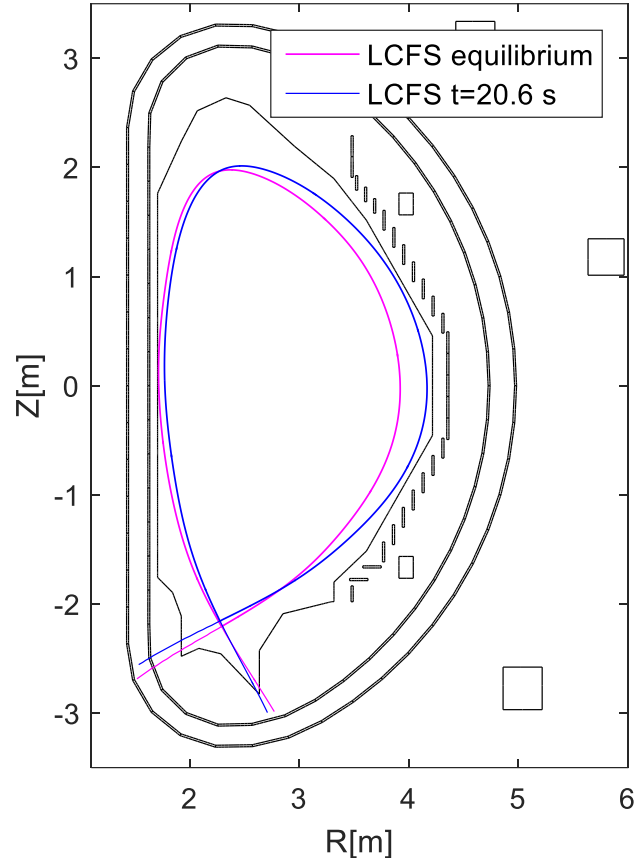


**FIGURE 26. MAXIMUM DEVIATION IN PLASMA SHAPE, WHEN THE ITER-LIKE MINOR DISRUPTION IS  
CONSIDERED AND 19 FLUXES ARE CONTROLLED.**

#### 4.2.2 Response to a change in shape

As an additional test scenario for closed-loop simulations with CCS, the case of a change in the plasma shape has been also considered. In this case the isoflux XSC-like plasma shape controller that feeds back the 8 control points shown in Figure 17, has been used to track a change in the required shape from the dashed black shape to the dashed red one shown in Figure 27. The transition time from the initial shape to the target was set equal to 1.5 s. It can be noticed that the controller is able to track the required shape with negligible error (at steady-state). Figure 28 shows the time traces for the fluxes at the 8 control points, while Figure 29 shows the correspondent control errors.

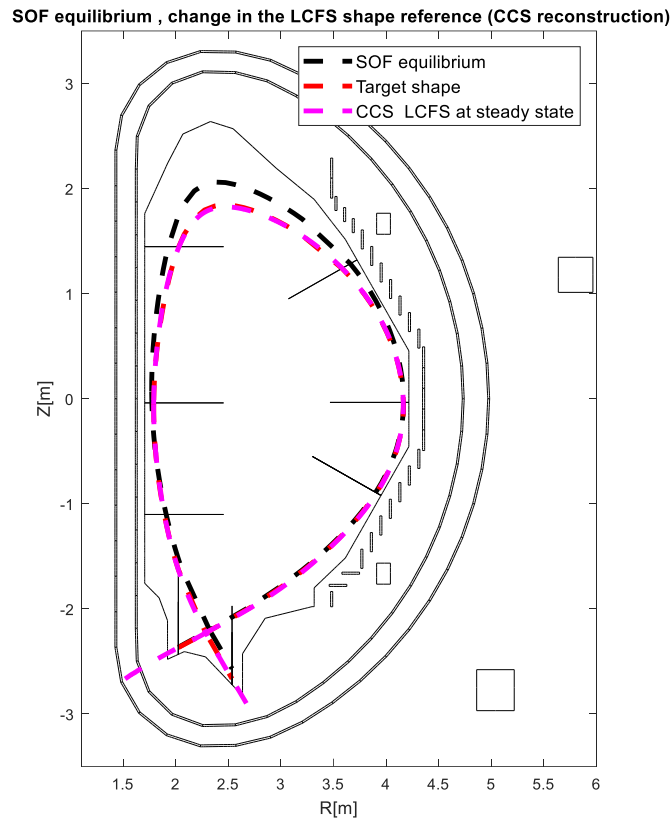


**FIGURE 27. RESPONSE OF THE XSC-LIKE ISOFLUX CONTROLLER TO A CHANGE OF SHAPE REQUEST. THE DASHED BLOCK SHAPE IS THE STARTING SHAPE, WHILE THE DASHED RED IS THE TARGET ONE. THE MAENTA DASHED SHAPE IS THE LCFS AT STEADY STATE.**

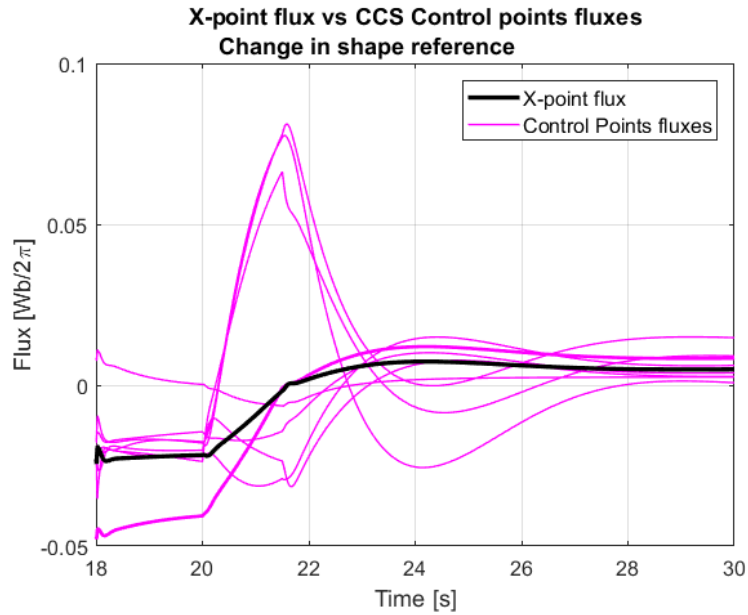


**FIGURE 28. COMPARISON BETWEEN THE FLUX AT THE X-POINT AND THE FLUXES AT THE 8 CONTROL POINTS RECONSTRUCTED BY THE CCS ALGORITHM, WHEN THE SHAPE REFERENCE IS CHANGING BETWEEN 20 s AND 21.5 s.**

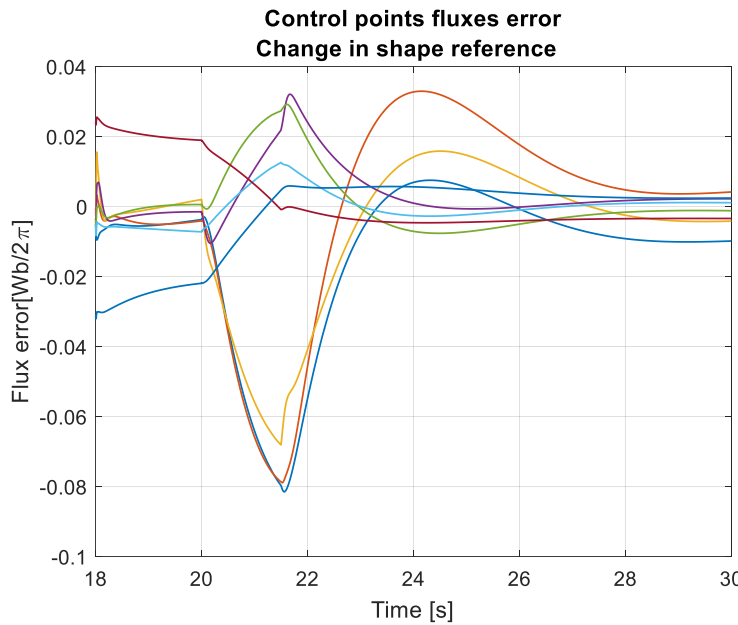


**FIGURE 29. FLUX CONTROL ERROR FOR THE CASE OF 8 CONTROL POINTS WHEN THE SHAPE REFERENCE IS CHANGING BETWEEN 20 S AND 21.5 S.**

#### 4.2.3 Preliminary assessment in presence of noise

JT-60U data have been used [9] to estimate the expected noise on the measurement.

A gaussian noise has been considered with standard deviation equal to

- $\sigma_{mp} = 0.05$  mT for the magnetic probes;
- $\sigma_{fl} = 0.025$  mWb for the flux loops;
- $\sigma_{PFC\%} = 0.075\%$  (relative standard deviation) for the currents in the PFC.

As a reference scenario to assess the effect of noise on plasma shape control, a minor disruption during Scenario 2 has been considered, by using the time traces of  $\beta_p$  and  $I_i$  shown in Figure 4, since this represent the worst considered scenario as summarized in the previous section.

It turned out that the expected noise does not have any practical impact on the controller performance, being the mean of the error on the plasma boundary reconstruction in the order of  $10^{-3}$  cm. As an example, for the considered simulation, the mean of the reconstruction error on the vertical and horizontal position of the X-point is equal to  $-2.7 \cdot 10^{-3}$  cm and  $8.4 \cdot 10^{-4}$  cm, respectively.

## 5. Integration of the QST magnetic (FBC) controller and CCS reconstruction to the CREATE model of JT60

The QST controller isoflux controller, also referred in this document as FBC, controls plasma current, position and shape using an isoflux control scheme. It calculates command values of active coil currents based on proportional-integral (PI) feedback control for the CS1, CS2, CS3, CS4, EF1, EF2, EF3, EF4, EF5 and EF6 PFC. Moreover, it uses a proportional-derivative (PD) feedback control for the FPPC1 and FPPC2 in-vessel coils.

The CREATE XSC-like isoflux controller and the  $/p$  controller used to track both plasma shape and current references in closed-loop simulations described in Sections 3 and 4, were replaced with the FBC controller. The response of the plasma and circuits is simulated using the CREATE linear model, whose outputs are fed into the CCS code to reconstruct the fluxes needed by FBC. This section summarizes the results of the simulation obtained with this setup, when the minor disruption defined in [1] is applied. The simulation was carried out with a sampling time of 5 ms.

As it is shown in Figure 30, it has been proved that the FBC successfully controls the plasma shape. The flux at the control points and the correspondent flux errors are shown in Figure 31 and Figure 32, respectively.

The FBC gains used for the considered closed-loop simulation are reported in Table 3, while the original values provided by QST are reported in Table 2. It can be noticed that, with the only exception of the FPPC gains, the same values have been used for the considered closed-loop simulation. The slight difference in the FPPC gains is somehow expected, since the considered plasma/circuits response relies on a linear approximation. However, this result proves that the FBC control architecture is robust enough to cope with unavoidable plant uncertainties. Indeed, only a fine tuning of the gains was necessary to run the closed-loop simulation with the CREATE plasma/circuit linearized model.

**TABLE 2 ORIGINAL VALUES OF THE FBC CONTROL GAINS FOR PLASMA POSITION, SHAPE AND CURRENT (GAINS FBC\_V3.PDF)**

| Shaping Gains (GSP, GSI) |                         | Xp flux Gains (GXP, GXI) |                         | FPPC Gains (GFP, GFD) |                         |
|--------------------------|-------------------------|--------------------------|-------------------------|-----------------------|-------------------------|
| GSP<br>(proportional)    | GSI [1/s]<br>(integral) | GXP<br>(proportional)    | GXI [1/s]<br>(integral) | GFP<br>(proportional) | GFD [s]<br>(derivative) |
| 0.5                      | 3.0                     | 1.0                      | 10.0                    | 0.0                   | 0.005                   |

**TABLE 3 CONTROL GAINS FOR PLASMA POSITION, SHAPE AND CURRENT SET IN THE REFERENCE.DAT FILE FOR THE CONSIDERED CLOSED-LOOP SIMULATION OF THE FBC CONTROLLER WITH THE CREATE PLASMA LINEAR MODEL.**

| Shaping Gains (GSP, GSI) |                         | Xp flux Gains (GXP, GXI) |                         | FPPC Gains (GFP, GFD) |                         |
|--------------------------|-------------------------|--------------------------|-------------------------|-----------------------|-------------------------|
| GSP<br>(proportional)    | GSI [1/s]<br>(integral) | GXP<br>(proportional)    | GXI [1/s]<br>(integral) | GFP<br>(proportional) | GFD [s]<br>(derivative) |
| 0.5                      | 3.0                     | 1.0                      | 10.0                    | 0.125                 | 0.015                   |

**SOF equilibrium with a Minor Disruption (FBC control)**

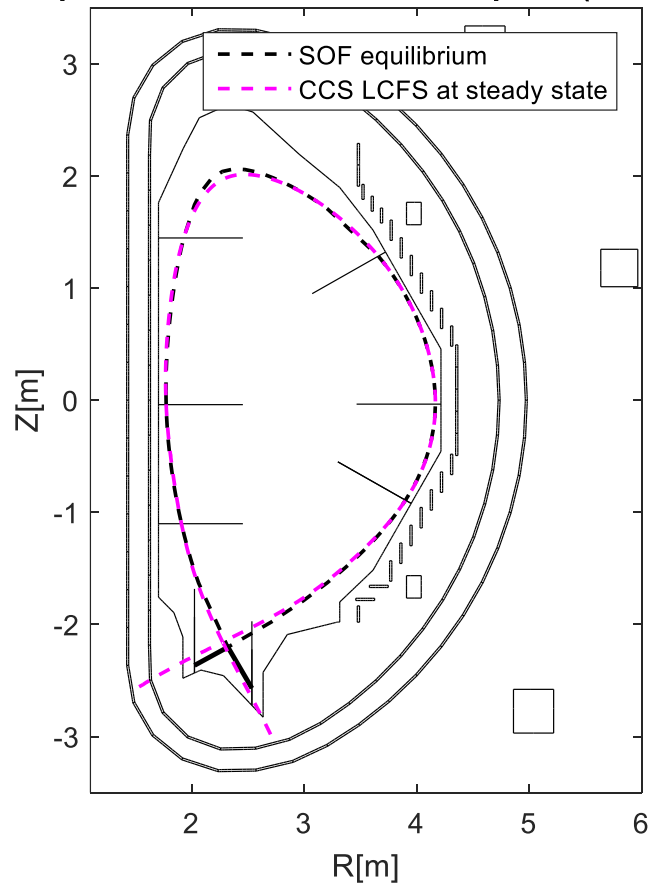


**FIGURE 30 COMPARISON BETWEEN THE REFERENCE SHAPE (I.E., THE SHAPE AT THE CONSIDERED EQUILIBRIUM) AND THE LCFS RECONSTRUCTED BY THE CCS CODE AT STEADY-STATE IN THE PRESENCE OF A MINOR DISRUPTION WHEN FBC IS USED TO CONTROL THE PLASMA.**

**X-point flux vs. Control points fluxes (CCS reconstruction FBC control)**

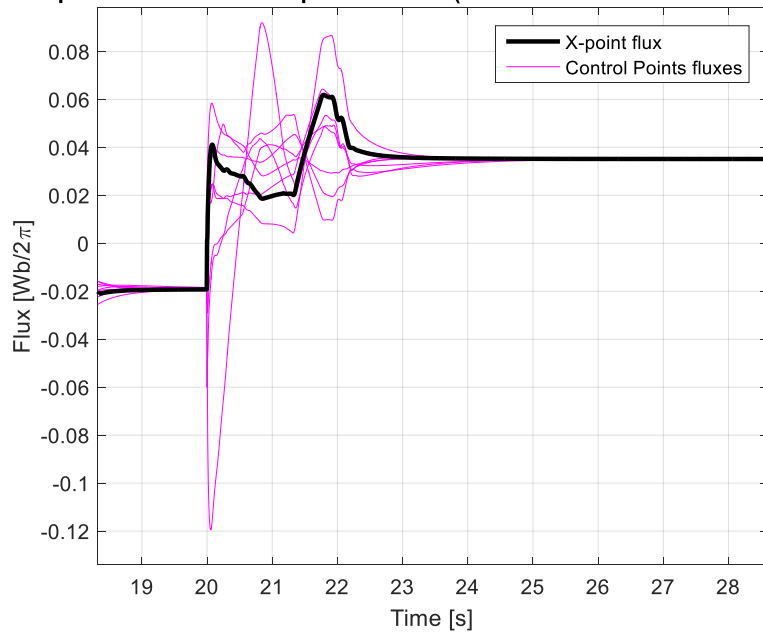


**FIGURE 31 COMPARISON BETWEEN THE FLUX AT THE X-POINT AND THE FLUXES AT THE 8 CONTROL POINTS RECONSTRUCTED BY THE CCS ALGORITHM WHEN THE FBC IS USED TO REJECT A MINOR DISRUPTION APPLIED AT T= 20 s.**

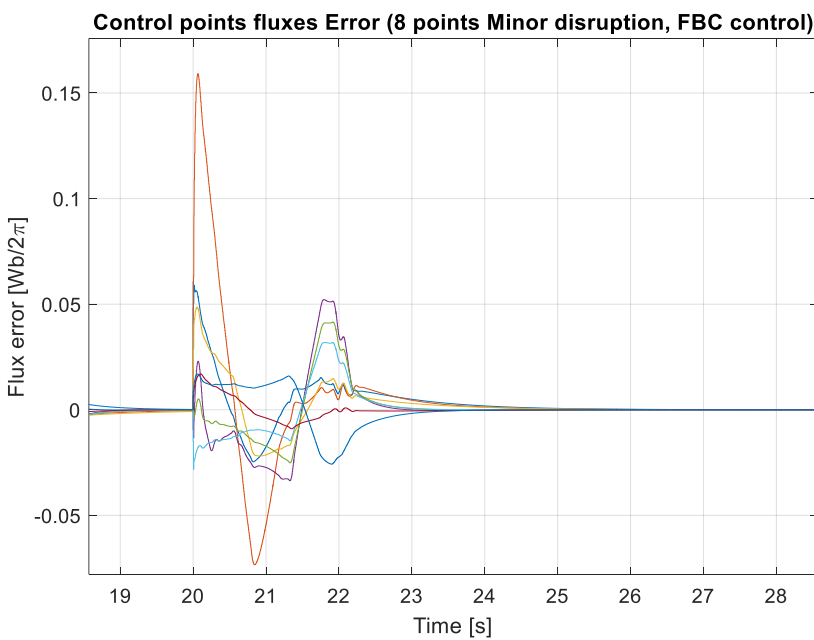


**FIGURE 32. FLUX CONTROL ERROR AT THE 8 CONTROL POINTS WHEN THE FBC IS USED TO REJECT A MINOR DISRUPTION APPLIED AT T=20 s.**

## 6. References

- [1] B. Spears, "JT-60SA Plant Integration Document (v 3.8)".
- [2] N. Cruz et al., "Control-oriented tools for the design and validation of the JT-60SA," *Control Engineering Practice*, vol. 63, pp. 81-90, 2017.
- [3] D. Corona et al., "Plasma shape control assessment for JT-60SA using the CREATE tools," *Fusion Engineering and Design*, vol. 146, pp. 1773-1777, 2019.
- [4] H. Urano, et al., "Development of operation scenarios for plasma breakdown and current ramp-up phases in JT-60SA tokamak," *Fusion Engineering and Design* 100 (2015) 345–356.
- [5] CREATE Team, "Plasma Position and Shape Control for ITER Scenarios," technical report on EFDA Study Contract 07\_1702/1579 (TW6\_TPO\_PLASMADYN1), December 2007.
- [6] A. Loarte, "Summary of Kick-off Meeting for tasks TW6-TPO-DISLOAD and TW6-TPO-PLASMADYN," July 2007.
- [7] Y. Miyata, T. Suzuki, S. Ide, H. Urano, "Study of Plasma Equilibrium Control for JT-60SA using MECS," *Plasma Fusion Research* 9 (2014) 3403045–3403055.
- [8] Y. Miyata, et al., "Study of JT-60SA Operation Scenario using a Plasma Equilibrium Control Simulator," *Plasma Fusion Research* 8 (2013) 2405109–2405109.
- [9] Y. Miyata et al., "Investigation of methods for mitigating influences of magnetic measurement noises on equilibrium control in JT-60SA", IAEA Tech. Meeting, 2017.